Astronomy & Astrophysics

L ETTER TO THE E DITOR

Redshift evolution of the Amati relation: Calibrated results from the Hubble diagram of quasars at high redshifts

Yan Dai (戴岩)[1,2], Xiao-Gang Zheng (郑晓刚)[3], Zheng-Xiang Li (李正祥)[1],
He Gao (高鹤)[1], and Zong-Hong Zhu (朱宗宏)[1]

[1] Department of Astronomy, Beijing Normal University, Beijing 100875, PR China
e-mail: zxli918@bnu.edu.cn, gaohe@bnu.edu.cn, zhuzh@bnu.edu.cn
[2] Beijing Planetarium, Beijing 100044, PR China
[3] School of Electrical and Electronic Engineering, Wuhan Polytechnic University, Wuhan 430023, PR China

ABSTRACT

Gamma-ray bursts (GRBs) have long been proposed as a complementary probe to type Ia supernovae (SNe Ia) and the cosmic microwave background to explore the expansion history of the high-redshift universe, mainly because they are bright enough to be detected at greater distances. Although they lack definite physical explanations, many empirical correlations between GRB isotropic energy or luminosity and some directly detectable spectral or temporal properties have been proposed to make GRBs standard candles. Since the observed GRB rate falls off rapidly at low redshifts, this thus prevents a cosmology independent calibration of these correlations. In order to avoid the circularity problem, SN Ia data are usually used to calibrate the luminosity relations of GRBs in the low redshift region (limited by the redshift range for SN Ia sample), and then they are extrapolate the luminosity relations to the high redshift region. This approach is based on the assumption of no redshift evolution for GRB luminosity relations. In this work, we suggest the use of a complete quasar sample in the redshift range of $0.5 < z < 5.5$ to test such an assumption. We divided the quasar sample into several subsamples with different redshift bins, and used each subsample to calibrate the isotropic γ-ray equivalent energy of GRBs in relevant redshift bins. By fitting the newly calibrated data, we find strong evidence that the most commonly used Amati relation between spectral peak energy and isotropic-equivalent radiated energy shows no, or marginal, evolution with redshift. Indeed, at different redshifts, the coefficients in the Amati relation could have a maximum variation of 0.93% at different redshifts, and there could be no coincidence in the range of 1σ.

Key words. gravitational waves – stars: neutron – stars: oscillations – quasars: general

1. Introduction

As the most intense explosions in the universe, gamma-ray bursts (GRBs) are bright enough to be detected in the high-redshift range up to at least $z \sim 10$ (Tanvir et al. 2009; Salvaterra et al. 2009), so that GRBs have been widely discussed as a complementary probe to type Ia supernovae (SNe Ia) and the cosmic microwave background (CMB) to explore the expansion history of the high-redshift universe (Amati & Della 2013; Wang et al. 2015, for a review). In order to make GRBs standard candles, many empirical correlations between their isotropic energy or luminosity and some directly detectable spectral or temporal properties have been proposed. For instance, Amati et al. (2002) discovered a correlation between the isotropic bolometric emission energy ($E_{\rm iso}$) and the rest-frame peak energy ($E_{{\rm p},z}$), later Ghirlanda et al. (2004a) proposed that there exists an even tighter correlation between $E_{{\rm p},z}$ and the beaming-corrected bolometric emission energy (E_γ). In order to reduce the scatter of the correlations, several multiple relations have also been proposed, such as the $E_{\rm iso} - E_{{\rm p},z} - t_{{\rm b},z}$ relation (Liang & Zhang 2005), among others (see more correlations reviewed in Ghirlanda et al. 2004b; Demianski et al. 2017a; Zhang 2018).

These GRB luminosity indicators have been widely used as standard candles for cosmology research (Schaefer 2007;

Wang et al. 2007, 2017; Amati et al. 2008, 2019; Amati & Della 2013; Wei et al. 2013; Muccino et al. 2021; Montiel et al. 2021), and it has been shown that when combined with other probes, GRBs can indeed extend the Hubble diagram to higher redshifts and help to make better constraints on cosmological parameters (Amati & Della 2013; Wang et al. 2015, for a review). However, since the observed GRB rate falls off rapidly at low redshifts, it is very difficult to make a robust calibration for those GRB correlations. Normally, a robust cosmology independent calibration (e.g., the standard ΛCDM cosmology) would be used to calculate the isotropic energy or luminosity for GRB samples and then used to derive the empirical correlations. As a result, the so-called circularity problem could prevent the direct use of GRBs for cosmology.

To avoid the circularity problem, it has been proposed to use SN Ia data in the same redshift range as GRBs to calibrate their luminosity correlations (Liang et al. 2008; Vitagliano et al. 2010; Gao et al. 2012). Considering that objects at the same redshift should have the same luminosity distance in any cosmology, one can assign the distance moduli of SN Ia to GRBs at the same redshifts (Liang et al. 2008; Demianski et al. 2017a), or one can use the SN Ia data to fit the model-independent cosmography formula that reflects the Hubble relation between the luminosity distance and redshift, and then obtain the GRB luminosity

distance (Gao et al. 2012; Amati et al. 2019). In this way, one can derive a cosmology-independent calibration for the GRB candles.

The shortage of using SN Ia to calibrate GRB correlations is that the redshift range of SN Ia data is relatively low. In this case, one can only calibrate the correlations for the low redshift GRB sample and extend the calibrated relations to high redshift. For this method, one needs to make a hypothesis that there is no evolution with respect to redshift for the GRB correlations. It is of great interest and necessary to test this hypothesis because the high redshift GRB samples are the most important for the study of cosmology.

Recently, based on a nonlinear relation between quasars' UV and X-ray luminosities, (parametrized as $\log(L_X) = \gamma \log(L_{UV}) + \beta$), Risaliti & Lusso (2019) constructed a Hubble diagram of quasars in the redshift range of $0.5 < z < 5.5$, which is in excellent agreement with the analogous Hubble diagram for SNIa in the redshift range of $0.5 < z < 1.4$. Here we suggest dividing the quasar sample into several subsamples with different redshift bins, and we used each sample to calibrate GRB correlations to test if there exists redshift evolution for these relations.

2. Amati relation and GRB sample

Although, many empirical luminosity correlations have been statistically found from long GRB observations, the Amati correlation is the most widely used one for cosmological studies. In this work, we focus on the discussion regarding the redshift dependence of the Amati relation. This relation was first found for a sample of long GRBs detected by *Beppo*SAX with known redshifts (Amati et al. 2002; Amati 2006), showing that more energetic GRBs tend to be spectrally harder. With the increase of long GRB events, the Amati relation always holds, although a few significant outliers do exist (Amati et al. 2008). Thanks to the successful operation of the *Neil Gehrels Swift* Observatory (Gehrels et al. 2004), a good sample of short GRBs were well localized, whose redshifts were precisely measured. It is found that short GRBs also have the correlation between the isotropic bolometric emission energy and the rest-frame peak energy, but they seem to form a parallel track above the long-GRB Amati relation (Ghirlanda et al. 2009). For this work, we only focus on the long GRB sample.

The Amati relation has the following form:

$$\frac{E_{p,z}}{100\,\text{keV}} = C \left(\frac{E_{iso}}{10^{52}\text{erg}}\right)^m \tag{1}$$

with $C \sim 0.8-1$ and $m \sim 0.4-0.6$ (Amati 2006). We note that E_{iso} is the isotropic equivalent energy in the gamma-ray band, which can be calculated from the bolometric fluences S_{bol} as

$$E_{iso} = 4\pi d_L^2 S_{bol} (1 + z)^{-1} , \tag{2}$$

where S_{bol} is calculated from the observed fluence in the rest frame $1-10\,000$ keV energy band by assuming the Band function spectrum (Band et al. 1993)

$$N(E) = \begin{cases} A \left(\frac{E}{100\,\text{keV}}\right)^\alpha \exp\left(\frac{E}{E_0}\right), & E < (\alpha - \beta)E_0 \\ A \left(\frac{(\alpha-\beta)E_0}{100\,\text{keV}}\right)^\alpha \exp(\alpha - \beta)\left(\frac{E}{100\,\text{keV}}\right)^\beta, & E > (\alpha - \beta)E_0 \end{cases} \tag{3}$$

where $E_{p,z} = (1 + z)E_p$ is the rest-frame peak energy, and $E_p = (\alpha + 2)E_0$ is the peak energy in the $E^2 N(E)$ spectrum.

For the purpose of this work, we express the Amati relation as

$$\log\left(\frac{E_{p,z}}{\text{keV}}\right) = a \log\left(\frac{E_{iso}}{\text{erg}}\right) + b. \tag{4}$$

Here we adopt the GRB sample compiled in Demianski et al. (2017a,b), which includes 162 well-measured GRBs in the following redshift range: $z \in [0.125, 9.3]$. We divided the GRB sample into four sub-groups with different redshift bins, for example, $0.125 < z \le 1$, $1 < z \le 2$, $2 < z \le 3$, and $z > 3$. The number of GRBs contained in the four subsamples is 42, 54, 35, and 30, respectively.

3. Calibration results for Amati relation using Hubble diagram of quasars

As the most luminous persistent sources in the Universe, quasars are bright enough to be detected up to redshifts $z > 7$ (Mortlock et al. 2011; Banados et al. 2018; Wang et al. 2018; Yang et al. 2020). According to the currently accepted model, quasars are extremely luminous active galactic nuclei (AGNs), where the observed intense energy release are related to the accretion of a gaseous disk onto a supermassive black hole (SMBH). Quasars have a wide spectral energy distribution, which normally contains a significant emission component in the optical-UV band L_{UV}, the so-called big blue bump, with a softening at higher energies (Sanders et al. 1989; Elvis et al. 1994; Trammell et al. 2007; Shang et al. 2011). It has long been discussed that there is a nonlinear relationship between L_{UV} and the quasar's X-ray luminosity L_X, parametrized as $\log(L_X) = \gamma \log(L_{UV}) + \beta$ (Vignali et al. 2003; Strateva et al. 2005; Steffen et al. 2006; Just et al. 2007; Green et al. 2009; Young et al. 2010; Jin et al. 2012). From the theoretical point of view, this relation could be intrinsic since the UV emission is usually thought to originate from the optically thick disk surrounding the SMBH and the X-ray photons are thought to be generated through the inverse-Compton scattering of these disk UV photons by a plasma of hot relativistic electrons (the so-called corona) around the accretion disk. Such a relation is found to be independent of redshift (Lusso & Risaliti 2016), so that it could be used as a distance indicator to estimate cosmological parameters. The initial dispersion of the $L_{UV} - L_X$ relation is relatively large ($\delta \sim 0.35-0.4$, Just et al. 2007; Young et al. 2010), but after a detailed study, Lusso & Risaliti (2016) suggest that most of the observed dispersion is not intrinsic, but it is rather due to observational effects. By gradually refining the selection technique and flux measurements, Risaliti & Lusso (2019) collected a complete sample of quasars, whose dispersion of the $L_{UV} - L_X$ relation is smaller than 0.15 dex. The sample of main quasars is composed of 1598 data points in the range from $0.036 < z < 5.1$. With this sample, they constructed a Hubble diagram of quasars in redshift range of $0.5 < z < 5.5$, which is in excellent agreement with the analogous Hubble diagram for SNIa in the redshift range of $0.5 < z < 1.4$. Moreover, this Hubble diagram of quasars has been studied in cosmological applications (Zheng et al. 2020, 2021). Considering that objects at the same redshift should have the same luminosity distance in any cosmology, here we first fit the model-independent cosmography formula that reflects the Hubble relation between the luminosity distance and redshif using the quasar sample, and then we obtained the distance moduli (also the luminosity distance) for GRBs at a given redshift with the best fit results.

It has long been proposed that the evolution of the universe could be described by pure kinematics, only relying on the

Table 1. Best fitting values of coefficient a and b for each sub-sample.

	a	b	δ
$0.125 < z \leq 1$	0.518 ± 0.036	24.90 ± 1.90	0.262 ± 0.022
$1 < z \leq 2$	0.502 ± 0.033	24.00 ± 1.80	0.220 ± 0.017
$2 < z \leq 3$	0.431 ± 0.048	20.20 ± 2.60	0.215 ± 0.020
$z > 3$	0.436 ± 0.035	20.50 ± 1.90	0.149 ± 0.021
Total	0.491 ± 0.017	23.48 ± 0.89	0.220 ± 0.010

assumption of the basic symmetry principles (the cosmological principle) that the universe can be described by the Friedmann-Robertson-Walker metric, but independent of any cosmology model (Weinberg 1972). In such a cosmography framework, the luminosity distance could be expressed as a power series in the redshift by means of a Taylor series expansion (Visser 2004)

$$d_L(z) = cH_0^{-1}\left\{ z + \frac{1}{2}(1-q_0)z^2 - \frac{1}{6}\left(1 - q_0 - 3q_0^2 + j_0 \right.\right.$$
$$\left. + \frac{kc^2}{H_0^2 a^2(t_0)}\right)z^3 + \frac{1}{24}\left[2 - 2q_0 - 15q_0^2 - 15q_0^3 + 5j_0 \right.$$
$$\left.\left. + 10q_0 j_0 + s_0 + \frac{2kc^2(1+3q_0)}{H_0^2 a^2(t_0)}\right]z^4 + \ldots \right\}, \quad (5)$$

where $k = -1, 0, +1$ corresponds to a hyperspherical, Euclidean, or spherical universe, respectively. The coefficients of the expansion are the so-called cosmographic parameters (e.g., Hubble parameters H, deceleration parameters q, jerk parameters j, and snap parameters s), which relate to the scale factor $a(t)$ and its higher order derivatives:

$$H \equiv \frac{\dot{a}(t)}{a(t)}, \quad (6)$$

$$q \equiv -\frac{1}{H^2}\frac{\ddot{a}(t)}{a(t)}, \quad (7)$$

$$j \equiv \frac{1}{H^3}\frac{a^{(3)}(t)}{a(t)}, \quad (8)$$

$$s \equiv \frac{1}{H^4}\frac{a^{(4)}(t)}{a(t)}. \quad (9)$$

All subscripts "0" indicate the present value of the parameters ($t = t_0$). In order to avoid the convergence of the series at high redshift and to better control the approximation induced by truncations of the expansions, Cattoën & Visser (2007) proposed to use an improved parameter $y = z/(1+z)$ to recast the d_L expression as

$$d_L(y) = \frac{c}{H_0}\left\{ y - \frac{1}{2}(q_0 - 3)y^2 + \frac{1}{6}\left[12 - 5q_0 + 3q_0^2 \right.\right.$$
$$\left. - (j_0 + \Omega_0)\right]y^3 + \frac{1}{24}\left[60 - 7j_0 - 10\Omega_0 - 32q_0 \right.$$
$$\left.\left. + 10q_0 j_0 + 6q_0\Omega_0 + 21q_0^2 - 15q_0^3 + s_0\right]y^4 + O(y^5) \right\}, \quad (10)$$

where Ω_0 is the total energy density. For the purpose of this work, here we fit the truncation of the d_L expression (for the flat universe $\Omega_0 = 1$) to the second order term with the quasar sample. Our best cosmographic fitting result is

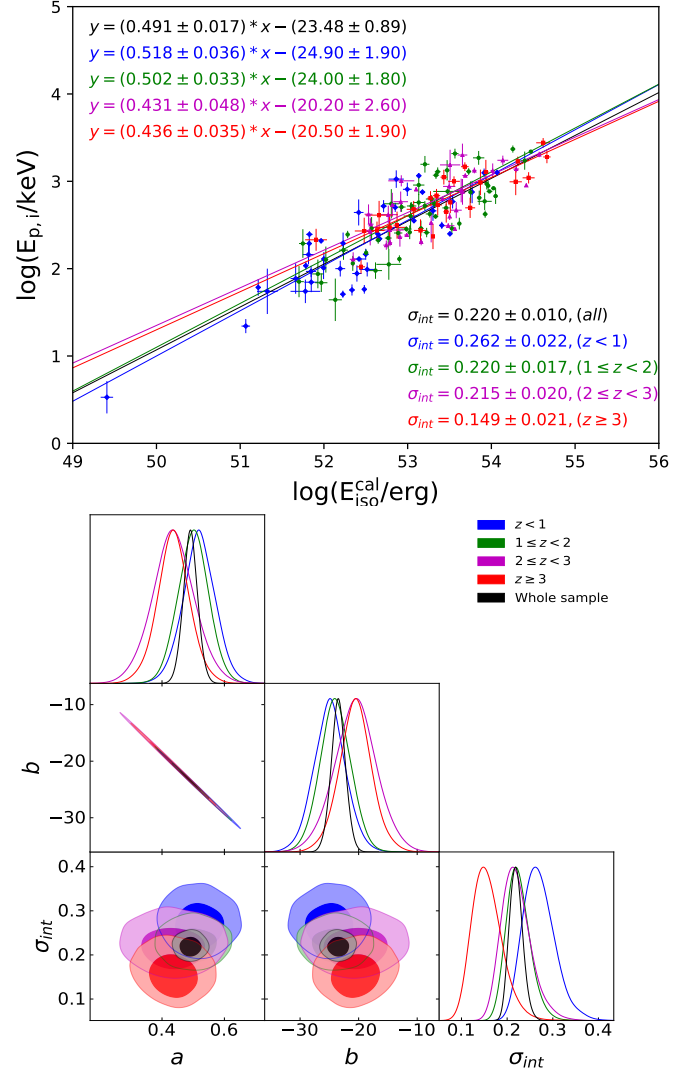$$q_0 = -0.64 \pm 0.61, \quad j_0 + \Omega_0 = 0.92 \pm 5.04.$$

Fig. 1. *Upper panel*: fitting results for Amati relation with GRB samples in different redshift range (the black line is for the whole sample, the blue line is for $0.125 < z \leq 1$, the green line is for $1 < z \leq 2$, the purple line is for $2 < z \leq 3$, and the red line is for $z \geq 3$), where the GRB distance moduli were calibrated by the quasar data. *Lower panel*: 1D marginalized distributions and 2D plots with 1σ and 2σ contours for luminosity correlation parameters.

In our adopted sample, 156 GRBs are in the redshift range of $0.5 < z < 5.5$. The luminosity distance for these GRBs were recalculated based on the best fitted cosmography formula, as was also the case for their isotropic equivalent energy in gamma-ray band.

With the newly calculated isotropic equivalent energy $E_{\rm iso}$, we calibrated the Amati relation for each subsample and the whole sample. Here we make a logarithm linear fitting between $E_{{\rm p},z}$ (in units of keV) and $E_{\rm iso}$ (in units of ergs) by adopting a likelihood function written as (Reichart et al. 2001)

$$L(a, b, \sigma) = \frac{1}{2}\frac{\sum \log (\sigma^2 + \sigma_{y_i}^2 + a^2\sigma_{x_i}^2)}{\log (1 + a^2)}$$
$$+ \frac{1}{2}\sum \frac{(y_i - ax_i - b)^2}{\sigma^2 + \sigma_{y_i}^2 + a^2\sigma_{x_i}^2}, \quad (11)$$

where $x_i = \log(E_{\rm iso})$, $y_i = \log(E_{{\rm p},z})$, and σ marks the observational intrinsic dispersion. We adopted the Python package of
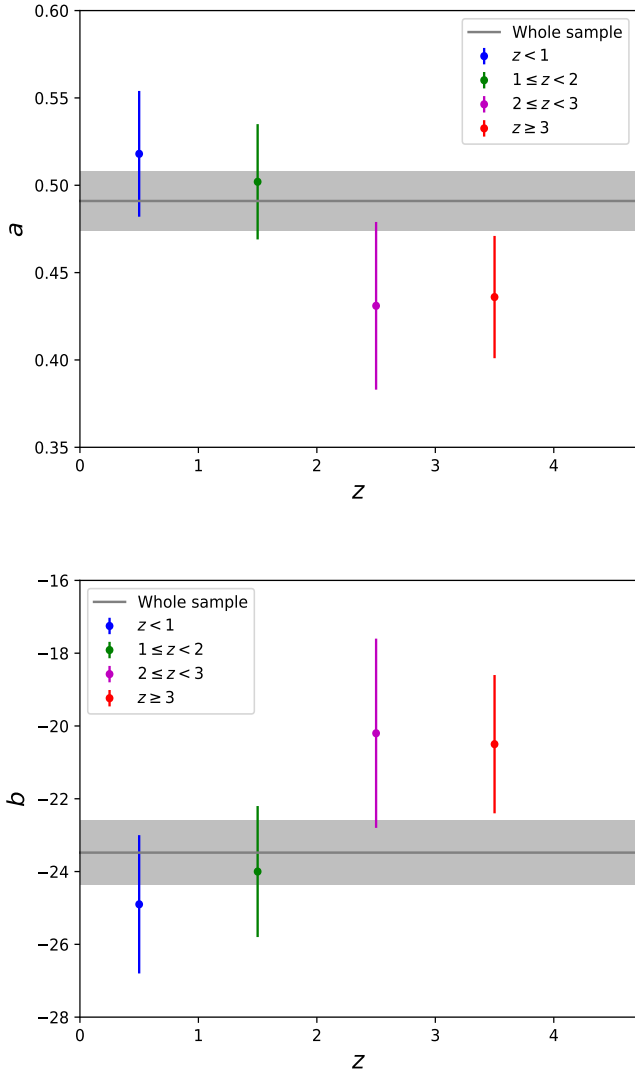
Fig. 2. Best fitting values of coefficient a (*upper panel*) and b (*lower panel*) for each subsample with respect to the subsample's mean redshift.

emcee to perform the fitting and took the Uniform priors on $a \in [0, 4]$, $b \in [50, 56]$, and $\delta \in [0, 1]$. The best fitting results for each subsample and the whole sample have been consolidated in Table 1 and plotted in Fig. 1. In the bottom panel of Fig. 1, we show the 1D marginalized distributions and 2D contours with the 1σ and 2σ confidence region. In Fig. 2, we plotted the best fitting values of coefficient a and b for each subsample with respect to the subsample's mean redshift.

Our results show that the best fitting values of a and b seem to have a certain redshift evolution. For coefficient a, the results of the first three subsamples ($z < 3$) are in good agreement with each other, however the result of the last high redshift subsample does not coincide with the previous ones in the range of 1σ. Even so, they still coincide in the range of 2σ. More interestingly, the best fitting values of coefficient b first increases and then decreases with the increase in the sample redshift. The variation range of the b value between different subsamples could reach 0.93%, and the result for the medium redshift range ($1 < z < 3$) does not coincide with the low or high redshift sample in range of 1σ. As shown in the lower panel of Fig. 1, parameters a and b are correlated, which is expected for a linear fit. There seems to

be no evolution trend for the dispersion (denoted by the δ value) of the relation.

4. Discussion

Gamma-ray bursts are attractive cosmic probes due to their high redshift characteristics. Many empirical correlations between their isotropic energy/luminosity and some directly detectable spectral or temporal properties have been proposed, intending to shape GRBs into standard candles. However, unlike the Type Ia SNe, all these GRB luminosity relations lack definite physical explanations, mainly because our knowledge of the progenitor, central engine, and jet composition for GRBs are still limited. In this case, before applying GRBs to explore the universe, the properties of these relations need to be further examined. For example, whether there is redshift evolution for these relations is something worth studying. Using a complete quasar sample with a large redshift span to calibrate the isotropic equivalent energy of GRBs, here we find no significant evidence that the Amati relation has an evolution with redshift. Some previous methods, such as calibrating the luminosity relations of GRBs in the low redshift region and then extrapolating that to the high redshift region, may be problematic. It is worth noticing that the dispersion of the Hubble diagram for our adopted quasar sample is relatively large, which may bring some uncertainty as to the distance calibration, as well as to the fitting results for the Amati relation. Nevertheless, the method we have discussed here is universal. In the future, when the quasar sample quality becomes better or when there are other, better distance indicator samples with a large redshift span, we will study the redshift evolution of the GRB luminosity relation in more detail.

References

Amati, L. 2006, MNRAS, 372, 233
Amati, L., & Della, V. 2013, Int. J. Mod. Phys. D, 22(14), 1330028
Amati, L., Frontera, F., Tavani, M., et al. 2002, A&A, 390, 81
Amati, L., Guidorzi, C., Frontera, F., et al. 2008, MNRAS, 391, 577
Amati, L., D'Agostino, R., Luongo, O., et al. 2019, MNRAS, 486, L46
Banados, E., Venemans, B., Mazzucchelli, C., et al. 2018, Nature, 553, 473
Band, D., Matteson, J., Ford, L., et al. 1993, ApJ, 413, 281
Cattoën, C., & Visser, M. 2007, Classical and Quantum Gravity, 24, 5985
Demianski, M., Piedipalumbo, E., Sawant, D., et al. 2017a, A&A, 598, A112
Demianski, M., Piedipalumbo, E., Sawant, D., et al. 2017b, A&A, 598, A113
Elvis, M., Wilkes, B. J., McDowell, J. C., et al. 1994, ApJS, 95, 1
Gao, H., Liang, N., & Zhu, Z.-H. 2012, Int. J. Mod. Phys. D, 21, 1250016-1
Gehrels, N., Chincarini, G., Giommi, P., et al. 2004, ApJ, 611, 1005
Ghirlanda, G., Ghisellini, G., & Lazzati, D. 2004a, ApJ, 616, 331
Ghirlanda, G., Ghisellini, G., Lazzati, D., et al. 2004b, ApJ, 613, L13
Ghirlanda, G., Nava, L., Ghisellini, G., et al. 2009, A&A, 496, 585
Green, P. J., Aldcroft, T. L., Richards, G. T., et al. 2009, ApJ, 690, 644
Jin, C., Ward, M., & Done, C. 2012, MNRAS, 422, 3268
Just, D. W., Brandt, W. N., Shemmer, O., et al. 2007, ApJ, 665, 1004
Khadka, N., & Ratra, B. 2020, MNRAS, 497, 263
Liang, E., & Zhang, B. 2005, ApJ, 633, 611
Liang, N., Xiao, W. K., Liu, Y., et al. 2008, ApJ, 685, 354
Lusso, E., & Risaliti, G. 2016, ApJ, 819, 154
Montiel, A., Cabrera, J. I., & Hidalgo, J. C. 2021, MNRAS, 501, 3515
Mortlock, D., Warren, S., Venemans, B., et al. 2011, Nature, 474, 616
Muccino, M., Izzo, L., Luongo, O., et al. 2021, ApJ, 908, 181
Reichart, D. E., Lamb, D. Q., Fenimore, E. E., et al. 2001, ApJ, 552, 57
Risaliti, G., & Lusso, E. 2019, Nat. Astron., 3, 272
Salvaterra, R., Della Valle, M., Campana, S., et al. 2009, Nature, 461, 1258

Sanders, D. B., Phinney, E. S., Neugebauer, G., et al. 1989, ApJ, 347, 29
Schaefer, B. E. 2007, ApJ, 660, 16
Shang, Z., Brotherton, M. S., Wills, B. J., et al. 2011, ApJS, 196, 2
Steffen, A. T., Strateva, I., Brandt, W. N., et al. 2006, AJ, 131, 2826
Strateva, I. V., Brandt, W. N., Schneider, D. P., et al. 2005, AJ, 130, 387
Tanvir, N. R., Fox, D. B., Levan, A. J., et al. 2009, Nature, 461, 1254
Trammell, G. B., Vanden Berk, D. E., Schneider, D. P., et al. 2007, AJ, 133, 1780
Vignali, C., Brandt, W. N., & Schneider, D. P. 2003, AJ, 125, 433
Visser, M. 2004, Classical Quantum Gravity, 21, 2603
Vitagliano, V., Xia, J.-Q., Liberati, S., et al. 2010, J. Cosmol. Astropart. Phys., 2010, 005
Wang, F. Y., Dai, Z. G., & Zhu, Z.-H. 2007, ApJ, 667, 1
Wang, F. Y., Dai, Z. G., & Liang, E. W. 2015, New Astron. Rv., 67, 1
Wang, G.-J., Yu, H., Li, Z.-X., et al. 2017, ApJ, 836, 103
Wang, F.-G., Yang, J.-Y., Fan, X.-H., et al. 2018, ApJ, 869, L9
Wei, J.-J., Wu, X.-F., & Melia, F. 2013, ApJ, 772, 43
Weinberg, S. 1972, Gravitation and Cosmology: Principles and Applications of the General Theory of Relativity (Wiley-VCH), 688
Yang, J.-Y., Wang, F.-G., Fan, X.-H., et al. 2020, ApJ, 897, L14
Young, M., Elvis, M., & Risaliti, G. 2010, ApJ, 708, 1388
Zhang, B. 2018, The Physics of Gamma-Ray Bursts by Bing Zhang (Cambridge Univeristy Press), 2018
Zheng, X.-G., Liao, K., Marek, B., et al. 2020, ApJ, 892, 103
Zheng, X.-G., Cao, S., Biesiada, M., et al. 2021, Sci. China Phys. Mech. Astron., 64